ARTICLE   OPEN

Check for updates

Zea mays genotype influences microbial and viral rhizobiome community structure

Pooja Yadav[1], Amanda Quattrone[2,6], Yuguo Yang[1], Jacob Owens[1,7], Rebecca Kiat[1], Thirumurugen Kuppusamy[1], Sabrina E. Russo[1,3] and Karrie A. Weber [ID][1,4,5 ✉]

Plant genotype is recognized to contribute to variations in microbial community structure in the rhizosphere, soil adherent to roots. However, the extent to which the viral community varies has remained poorly understood and has the potential to contribute to variation in soil microbial communities. Here we cultivated replicates of two *Zea mays* genotypes, *parviglumis* and B73, in a greenhouse and harvested the rhizobiome (rhizoplane and rhizosphere) to identify the abundance of cells and viruses as well as rhizobiome microbial and viral community using 16S rRNA gene amplicon sequencing and genome resolved metagenomics. Our results demonstrated that viruses exceeded microbial abundance in the rhizobiome of *parviglumis* and B73 with a significant variation in both the microbial and viral community between the two genotypes. Of the viral contigs identified only 4.5% ($n = 7$) of total viral contigs were shared between the two genotypes, demonstrating that plants even at the level of genotype can significantly alter the surrounding soil viral community. An auxiliary metabolic gene associated with glycoside hydrolase (GH5) degradation was identified in one viral metagenome-assembled genome (vOTU) identified in the B73 rhizobiome infecting Propionibacteriaceae (Actinobacteriota) further demonstrating the viral contribution in metabolic potential for carbohydrate degradation and carbon cycling in the rhizosphere. This variation demonstrates the potential of plant genotype to contribute to microbial and viral heterogeneity in soil systems and harbors genes capable of contributing to carbon cycling in the rhizosphere.

ISME Communications; https://doi.org/10.1038/s43705-023-00335-4

INTRODUCTION

Plant roots create a carbon and nutrient-rich environment in soils supporting microbiota in the zone adjacent to the root epidermis, rhizoplane, and the soil adhering to plant roots, rhizosphere, or together referred to as the rhizobiome [1]. It is within this region where a diversity of microbiota including Bacteria, Archaea, Eukarya and viruses are recognized as members of the rhizobiome that can impact plant-soil-microbe interactions [2]. The microbial diversity of this environment has the potential to be impacted by viral infection where viral mediated cell lysis is recognized to impact microbial abundance in soils [3]. Viruses are abundant in soils ranging from 10^7 to 10^9 viruses g^{-1} of soil [4–6] and virus abundance can often exceed that of microbes [7]. To date a few studies have investigated virus abundance and predation in the rhizosphere [8, 9], but the impact of these processes in this dynamic region in soils remains poorly studied.

Virus infection can result in host cell lysis through a lytic or lysogenic infection thereby reducing host cell abundance. The lysis of these microbes results in the release of cell lysate which serves as an easily accessible carbon and nutrient source supporting the growth of other microbial members [10]. Hence, viral infections of microbial host cells can influence the metabolic functions of the microbial community. This may occur due to shifts in taxonomic composition and change in metabolic potential caused by differential viral predation or through the acquisition of auxiliary metabolic genes (AMGs) [11–15] resulting from viral infection. AMGs are viral genes acquired from their host, not required in viral replication but allow viruses to directly manipulate host metabolism [16]. Some well-known examples of AMGs acquired by viruses have been inferred to play a role in carbon [15], sulfur [17], and nitrogen [18] cycling. Together, these changes in relative abundance of microbial composition and introduction of functional genes like AMGs can alter the metabolic potential of microbial community by metabolically reprogramming their hosts, and/or expression of AMGs [9, 15, 19, 20]. While, the abundance of viruses in the rhizosphere has been reported before [8, 9, 21], the implication of viral impacts on the host abundance and metabolic potential remains understudied. Given the absence of universal marker genes across viruses, metagenomic studies are required to shed light on the role of viruses in the rhizobiome and, how viruses impact the abundance of the host cells, and their potential to reprogram host metabolism [22].

In the carbon-rich region surrounding the plant root, the rhizobiome community structure varies between plant species [23] and genotypes [24], owing to the influence of the plant, including variation in root exudate profiles [25]. The variation in

[1]School of Biological Sciences, University of Nebraska-Lincoln, Lincoln, NE, USA. [2]Complex Biosystems, University of Nebraska-Lincoln, Lincoln, NE, USA. [3]Center for Plant Science Innovation, University of Nebraska-Lincoln, Lincoln, NE, USA. [4]Department of Earth and Atmospheric Sciences, University of Nebraska-Lincoln, Lincoln, NE, USA. [5]Daugherty Water for Food Global Institute, University of Nebraska, Lincoln, NE, USA. [6]Present address: Texas A&M University, College Station, TX, USA. [7]Present address: University of Nebraska-Medical Center, Omaha, NE, USA. ✉email: kweber@unl.edu

root exudate profile secreted by host genotype and the resulting substrate-driven or bottom-up shifts in the microbial community structure are based on differential production of root exudates and community utilization [26, 27]. In addition to substrate driven controls on rhizobiome structure, viruses are recognized to infect microorganisms in the rhizosphere [8, 9]. Viruses require metabolically active hosts for replication and thus the patterns of viral communities are linked to active host cells [28–31]. While physiochemical heterogeneity in soils can alter viral abundance where it is recognized that soil moisture and pH can influence viral community structure [32–34], variation in plant roots also has the potential to contribute to viral community structure. In soils viruses impact host abundance and metabolic potential by infecting metabolically active organisms driving carbon-cycling [15, 35], and play a role in biogeochemical processes in the rhizosphere [9, 36]. The region surrounding the root is one where microorganisms are recognized to be metabolically active owing to the production of carbon-rich plant root exudates.

Here we test the hypothesis that both the microbial and viral rhizobiome community varies between two plant genotypes of one of the world's most important cereal crops, *Z. mays*, with recognized genetic diversity [37], *Z. mays* genotypes, *Z. mays ssp. parviglumis* (teosinte), wild congener, and *Z. mays* genotype B73 (hybrid of domesticated maize). Seeds of each genotype were sterilized, germinated under axenic conditions, and transplanted into a homogenized soil matrix and cultivated to an early vegetative (V4-V8) growth stage in a greenhouse under controlled conditions. Plants were harvested for phenotyping and rhizobiome samples were collected to enumerate cells and viruses as well as identify microbial community members in biological replicates using 16S rRNA gene amplicon sequencing and genome resolved metagenomics from DNA shotgun metagenome sequence data. Variation within the microbial and viral (DNA viruses) communities between *Z. mays* genotypes was statistically determined. The virus linked microbial hosts in the rhizobiome of the two genotypes rendered differences in host abundance. Assembled and annotated viral contigs were screened for functional genes defined as AMGs and included the potential to degrade carbohydrates. Together these data were assembled to determine variance and describe the microbial and viral rhizobiome community assemblage between the two selected *Z. mays* genotypes, *parviglumis* and B73.

MATERIALS AND METHODS
Seed source, germination, and *Z. mays* growth
Seeds of *Z. mays parviglumis* and B73 were obtained from the University of Nebraska, Lincoln in-house collection [38]. Twenty-four *parviglumis* and B73 seeds were sterilized and germinated under axenic conditions in sterilized petri-plates. From among the 24 seedlings, 12 seedlings were transplanted into 1.8 L pots containing homogenized sieved prairie soil mixed with autoclaved agricultural-field sandy-soil (60:40; mass/mass; Supplementary Information) [39]. Plants were cultivated in a greenhouse with an average 13-hour day length for 22 days at 31 °C with relative humidity between 60.2 and 97.6% consistent with the climate of the growing season in the Great Plains. Every three days plants were watered and fertilized with 25 mL of 25% Hoagland's solution [40]. Six biological replicates of each genotype at the same growth stage (V4-V8) were selected for harvesting. Growth stage was determined by the number of visible leaf collars.

Rhizobiome harvesting and sample collection
Plant roots and rhizobiome were harvested by gently cutting the pot to minimize soil and root disruption and carefully separated from bulk soil as previously described [38]. The roots were submerged in a known volume of sterile, nucleic acid and enzyme-free 1X phosphate buffered saline (PBS) and sonicated (Branson 450D, 30% amplitude, 0.3 s duty cycle) for one minute, three times at 30 s intervals [41, 42] to harvest the rhizoplane (microbiota attached to roots) as well as the rhizosphere (soil associated

with roots) and the final mass of the rhizobiome was determined. The rhizobiome suspension was centrifuged (800 X *g*). A known volume of the supernatant was filtered through 0.45 µm PVDF and 0.2 µm PVDF membrane and fixed with formaldehyde (0.5 v/v final concentration) for cell and virus enumeration [43, 44]. The remaining suspension was centrifuged (3000 × *g* for 10 min) and rhizobiome pellet was collected by another round of centrifugation at 10,000 × *g* for 20 min. Rather than discarding the supernatant, we proceeded with the collection of cells (and viruses) to ensure collection of small bacteria in the collected rhizobiome. The supernatant was strained through a 40 mm sterile cell strainer (Fisherbrand™ product #22363547) to remove plant cells and root debris and was collected on 0.2 µm polycarbonate membranes (product #GTTP04700) through vacuum filtration (≤ 2.5 bar). The membrane and pellet were flash frozen in liquid nitrogen and stored at −80 °C and the final rhizobiome was assembled from nucleic acid extracts. Following rhizobiome collection root phenotype characteristics were determined (Supplementary Information).

Nucleic acid extraction, 16S rRNA gene amplicon, and shotgun metagenomic sequence library preparation
All reagents and materials used in sample processing were treated or prepared in 0.1% diethylpyrocarbonate or RNase Away and autoclave sterilized. Nucleic acids were extracted from a known mass of the rhizobiome pellet (10% w/w of total rhizosphere and rhizoplane) and the membrane collected cells using a modified Griffith's method as previously described [44, 45]. DNA was quantified and purity was checked as previously described [44]. A quantified mass of DNA extracted from the pellet and the filter (2.5% of total DNA (ng)) were proportionally pooled to represent the total rhizobiome community. The DNA quantity was normalized per gram rhizosphere (Supplementary Information) and two technical replicates from each biological replicate (12 samples per genotype) were sent for 16S rRNA gene amplicon sequencing.

The 16S rRNA gene amplicon sequence library was prepared by the University of Minnesota Genomics Center, Minnesota using V4 and V5 regions of the 16S rRNA gene primers 515F and 806R as described [46, 47]. The samples were paired-end sequenced (2 × 300 bp) using Illumina MiSeq600 cycle v3 kit to a target sequencing depth of 72,000 reads per sample. The 16S rRNA gene amplicon sequence data was analyzed using the DADA2 package to obtain amplicon sequence variants (ASVs) as described [48] and calculate diversity measures (Supplementary Information). The ASVs were filtered for spurious sequences as described and was analyzed using phyloseq [49].

DNA extracted from three randomly selected biological replicates were submitted for shotgun metagenomic sequencing. The shotgun metagenome sequence library was prepared using the Nextera XT DNA library kit (Illumina, California, USA) as previously described [44]. The average final library size was 300 bp with an insert of 180 bp and a read length configuration of 150 PE for 40 M PE reads per sample (20 M in each direction). Sequence data were quality checked (Supplementary Information) and clean reads were used to generate de novo co-assemblies using Megahit [50]. Assembled contigs were binned using MetaBat2 (v2.15) [51], MaxBin2 (v2.2) [52], and CONCOCT (v1.1) [53] and dereplicated using DAS Tool (v1.1) [54]. The bins were quality checked using CheckM (v1.1) [55] and manually curated using Anvi'o (v7.0) [56] as described [44]. The final complete set of MAGs were taxonomically identified and used to estimate relative abundance as described (Supplementary Information).

Putative viral contigs were identified using VirSorter2 (v2.1) [57] and DeepVirFinder [58] followed by manual curation (Supplementary Information). A viral database was created to map the final set of viral contigs. A pairwise comparison with ≥95% average nucleotide identity (ANI) across ≥85% alignment coverage [59, 60] was used to assess genome similarity in the viral community of *parviglumis* and B73. All viral contigs greater than or equal to 1.5 Kbp were used in subsequent analyses. Viral contigs ≥10 Kbp are described as a vOTU [61]. A database was created from the dereplicated viral contigs and genome coverage of viral contigs was normalized as performed for MAGs and used as a proxy for relative abundance as previously described [15, 59, 62].

Virus-host linkages were established utilizing a combination of at least two of three different methods, clustered regularly interspaced short palindromic repeats (CRISPR) sequences [63], genome similarities [64], and tetranucleotide frequencies (threshold distance < 0.001) between host and viral contig (Supplementary Information) [15, 64–67]. Host genome metabolic potential determined using METABOLIC (v4.0) [68], DRAM (v1.2) [69], and FeGenie (v1.0) [70] at the MAG level. Viral contribution in
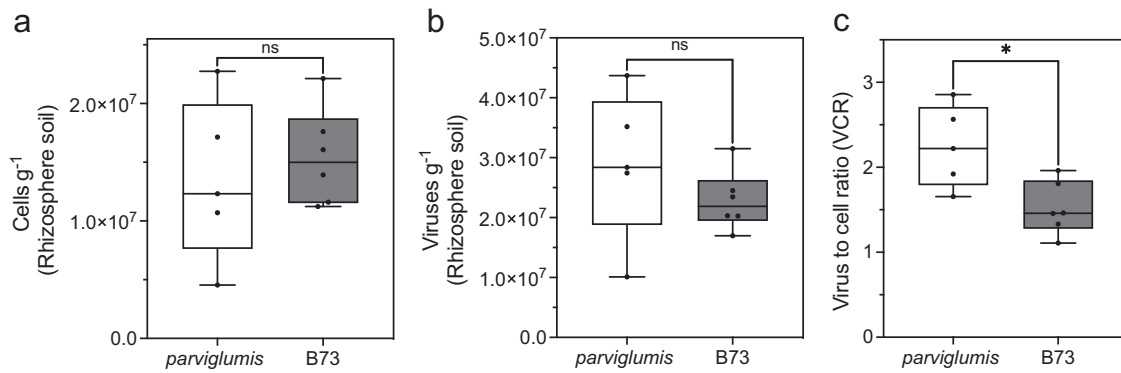
Fig. 1 Cell and virus abundance in the *parviglumis* and B73 rhizobiome. a Cell abundance per gram of soil in the rhizoplane and rhizosphere referred to a rhizobiome of biological replicates of *parviglumis* ($n = 5$) and B73 ($n = 6$). **b** Virus abundance per gram of the rhizobiome soil. **c** Virus to cell ratio (VCR) between *parviglumis* and B73. The boxes represent the interquartile range, the center represents the median, and the whiskers indicate ±1.5 times the interquartile range. A non-parametric unpaired t-test with Welch's correction assuming unequal variances was conducted. The asterisk denoted a *p* value < 0.05 as statistically significant whereas *ns* denoted that the result was not significant.

the host metabolic processes was investigated by screening assembled viral contigs for encoded putative AMGs in *parviglumis* and B73 using DRAM-v with flags flag-v, m with ranks of AMG confidence of 1 and 2.

Statistical analyses

All statistical analyses were conducted in R version 4.1.2 (2021-11-01). Differences between *Z. mays* genotypes in bacterial and virus abundances were tested using t-test assuming unequal variances. The correlation of cells and virus abundances were analyzed using Mantel's test and linear regression (Supplementary Information). Relationships between the microbial and viral community structure were analyzed using principal coordinate analysis (PCoA) with Bray-Curtis dissimilarities as implemented in the vegan package [71]. Differences between *Z. mays* genotypes in the microbial and viral community composition were evaluated using permutational multivariate analysis of variance (perMANOVA) using adonis2.

RESULTS

Virus to cell ratio in the *parviglumis* and B73 rhizobiome

Virus abundance exceeded cell abundance in the rhizobiome collected from *parviglumis* (VCR of 2.24 ± 0.21) and B73 (VCR 1.52 ± 0.12) and was positively correlated with cell abundance (Fig. 1). Cell abundance in the *parviglumis* and B73 rhizobiome totaled ($1.34 \pm 0.30 \times 10^7$ cells g^{-1}) and ($1.54 \pm 0.16 \times 10^7$ cells g^{-1}) respectively but was not statistically different between genotypes ($p > 0.05$, Fig. 1a). Similarly, rhizobiome virus abundance of *parviglumis* ($2.89 \pm 0.55 \times 10^7 g^{-1}$) and B73 ($2.28 \pm 0.20 \times 10^7 g^{-1}$) (Fig. 1b) exceeded cell abundance and was not statistically different between genotypes ($p > 0.05$). Cell and virus abundance did not differ significantly between genotypes, even when standardized by plant phenotypic parameters including root length, surface area, volume, density, fresh weight, or biomass (Supplementary Figs. S1, S2). Cell abundance g^{-1} of rhizobiome collected from *parviglumis* and B73 was positively correlated with the rhizosphere mass. While cell or virus abundance g^{-1} of rhizobiome collected was not statistically different between genotypes, the VCR significantly varied ($p = 0.02$) between genotypes indicating variation between genotypes.

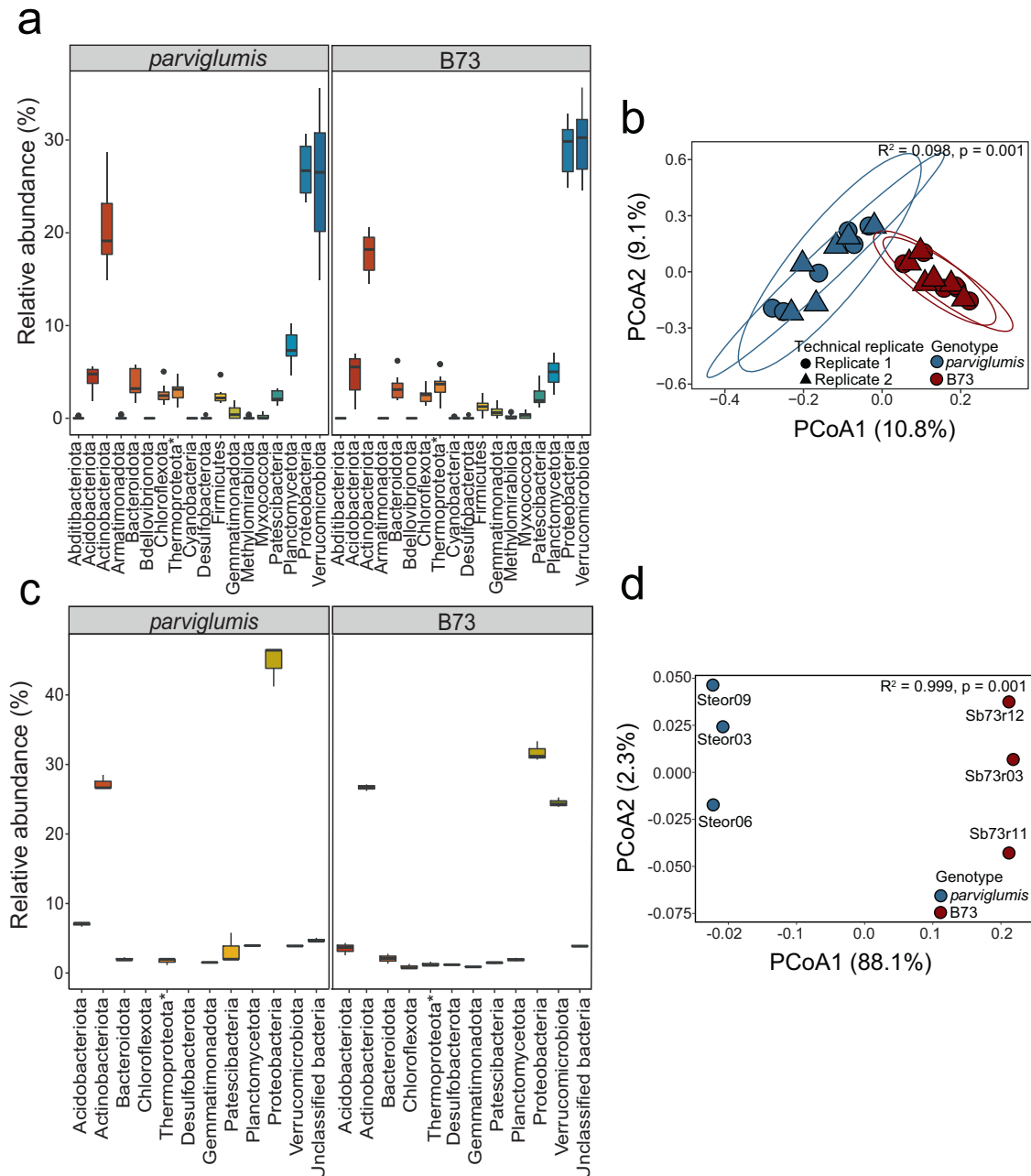#### Microbial community composition of *parviglumis* and B73 rhizobiome

The rhizobiome microbial community collected from the biological replicates of *parviglumis* and B73 revealed 6,317 unique ASVs from total ASVs identified (range 34,397–96,390) and (range 29,779–75,780) from clean reads of *parviglumis* and B73, respectively. The ASVs were broadly classified into 1 archaeal

phylum and 17 bacterial phyla (Fig. 2a). The rhizobiome common between genotypes consisted of Verrucomicrobiota, Proteobacteria, and Actinobacteriota with an abundance in similar proportions accounting for a combined 72.64% and 74.97% of the rhizobiome community in *parviglumis* and B73, respectively. The microbial community identified by 16S rRNA gene amplicon sequencing was statistically different between genotypes. (Fig. 2b; $R^2 = 0.098$, $p = 0.001$) where *Z. mays* genotype accounted for 10.8% of the variation in the microbial community structure (Fig. 2b).

Genome assembly of metagenomic sequence data resulted in MAGs similar to taxa identified at the ASV level where reads represented more than 2.5% of the microbial community (Fig. 2c). Biological replicates of the shotgun metagenome sequenced data yielded clean reads in the range of 22.85 to 24.12 million bps for *parviglumis* and 23.35 to 27.30 million bps for B73. These data rendered 50 and 61 rhizobiome metagenome-assembled genomes (MAGs) for *parviglumis* and B73, respectively. The *parviglumis* rhizobiome MAGs averaged $42.91 \pm 2.49\%$ completeness, totaling 15 medium-quality MAGs and 35 low-quality MAGs and B73 MAGs averaged estimated completeness of $43.60 \pm 2.23\%$, comprising one high-quality, 19 medium-quality, and 41 low-quality MAGs. All MAGs were included in additional analyses. Nine and 11 phyla in the archaeal and bacterial domains were identified in *parviglumis* and B73, respectively (Fig. 3). Similar to 16S rRNA sequencing data, the Thermoproteota was the only archaeal MAG reconstructed from the rhizobiome metagenomic sequence data obtained from both genotypes. The bacterial MAGs reconstructed from *parviglumis* rhizobiome were Acidobacteriota, Actinobacteriota, Bacteroidota, Desulfobacterota, Gemmatimondadota, Patescibacteria, Planctomycetota, Verrucomicrobiota, and unclassified bacteria. In addition to these taxa, two additional phyla, Chloroflexota and Desulfobacterota, were also reconstructed from B73 rhizobiome (Figs. 2c, 3).

As observed in 16S rRNA gene sequence data, taxa identified from MAGs revealed variance in the microbial community structure between genotypes (Fig. 2d; $p = 0.001$, $R^2 = 0.99$). The PCoA revealed 88.1% and 2.3% of the variance on axis 1 and 2, respectively (Fig. 2d). High variability of PCoA axis 1 demonstrated the variation in beta diversity between the two genotypes. This further highlighted the differences in the microbial community structure of *Z. mays* genotypes.

Similar to the 16S rRNA gene amplicon sequence data, MAGs also identified Proteobacteria and Actinobacteriota as the two most abundant rhizobiome phyla of both *parviglumis* and B73 rhizobiome (Fig. 3). Analyses of the B73 rhizobiome 16S rRNA gene

Fig. 2 Microbial community composition of *Z. mays parviglumis* and B73 identified by 16S rRNA gene amplicon sequence variants (ASVs) and metagenome-assembled genomes (MAGs). The microbial community of *parviglumis* and B73 represented (**a**) a percentage of the relative abundance of the microbial community identified by ASVs. **b** PCoA of ASVs identified in the rhizobiome collected from *parviglumis* (blue) and B73 (red) in biological and technical replicates with the Bray-Curtis distance matrix. The variance of (10.8%) on PCoA1 and (9.1%) on PCoA2 ($R^2 = 0.098$, *p*-value 0.001) as determined by perMANOVA. Ellipses denote 95% confidence intervals. **c** Relative abundance of MAGs determined using normalized genome coverage. **d** PCoA of MAG identified rhizobiome from *parviglumis* (blue) and B73 (red) with Bray-Curtis dissimilarities with 88.1% variance on PCoA1 and 2.3% variance on PCoA2 ($R^2 = 0.999$, $p = 0.001$). The box plot represents the interquartile range with whiskers ±1.5 times of interquartile range and the center depicts the median.

amplicon data revealed that in addition to taxa identified in the Proteobacteria and Actinobacteriota, Verrucomicrobiota taxa were abundant community members (Figs. 2a, c, 3). Within the Proteobacteria, community members in the family Xanthobacteraceae (18.00%) were the most abundant in the *parviglumis* rhizobiome. This result is different relative to the most abundant taxa identified at the family level in the B73 rhizobiome, where taxa within the Chthoniobacterales UBA10450 in the Verrucomicrobiota (16.39%) were the most abundant in B73 followed by Xanthobacteraceae (13.11%), Chloroflexota CSP1-4 (1.62%) and

Binatia UBA 9968 in Desulfobacterota (1.63%) (Figs. 2c, 3). In addition to microbial taxa, viral contigs were also identified from the shotgun metagenome sequence data (Fig. 3).

Rhizobiome viral community structure variation between *parviglumis* and B73

Identification of putative viruses from rhizobiome shotgun metagenome sequence data detected 329 and 488 viral contigs in *parviglumis* and B73, respectively. Further manual curation of viral contigs yielded 67 and 86 contigs with in the rhizobiome of
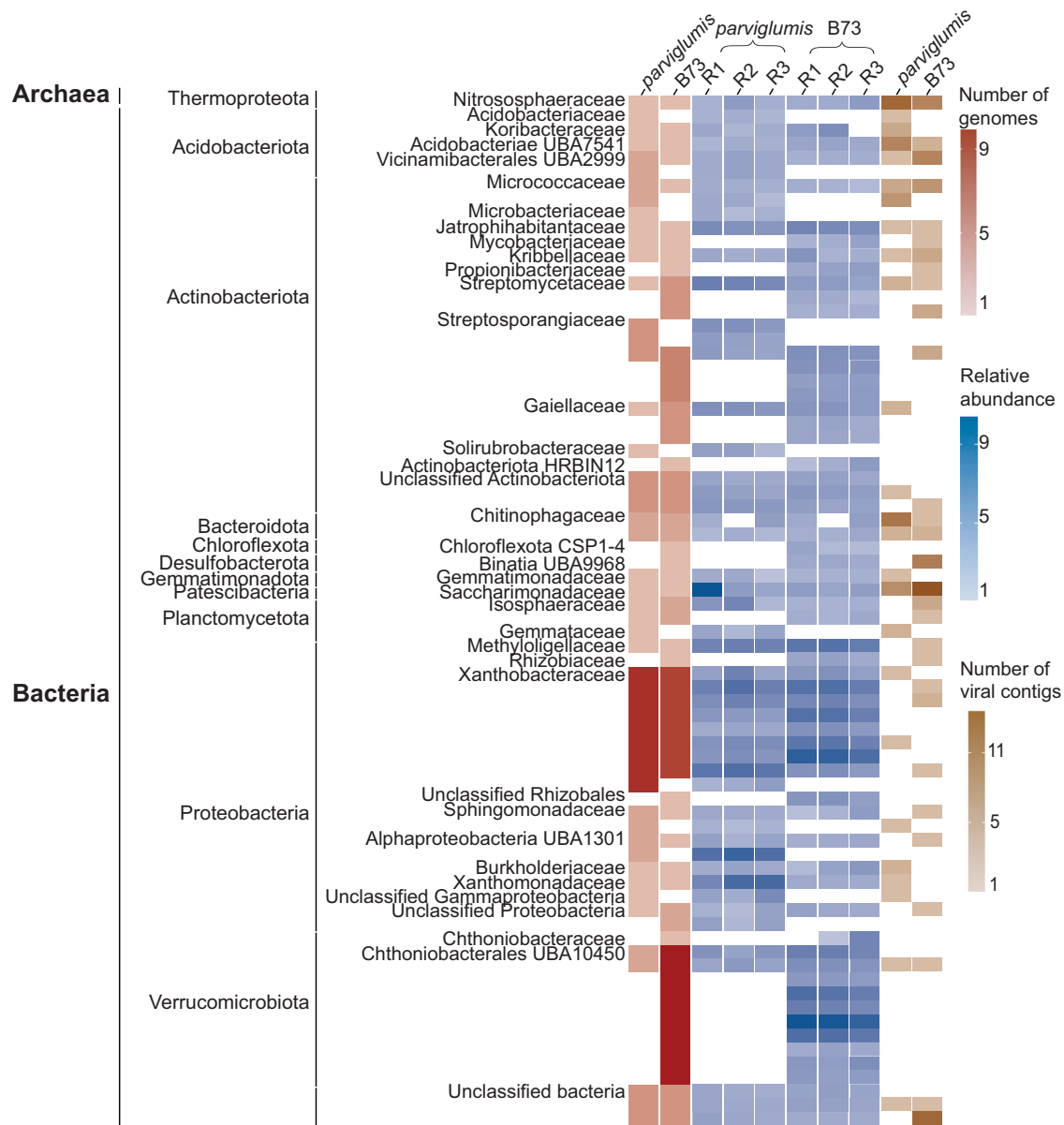
Fig. 3 Metagenome assembled genomes (MAGs) and viral contigs from the *Z. mays parviglumis* and B73 rhizobiome. MAGs were reconstructed and viral contigs were identified from three biological replicates from each genotype, *parviglumis* and B73 rhizobiome. The number of genomes corresponding to the archaeal and bacterial taxa classified by the GTDB database and clustered to the family level when possible is denoted in red and the relative abundance of genomes is denoted in blue. The mean coverage depth of MAGs normalized against the number of reads in the sample to calculate the relative abundance of the MAGs.

parviglumis and B73, respectively. The average nucleotide identity (ANI) distribution not only displayed a high level of strain heterogeneity but also revealed a wide range of viral genome variations. The size of putative viruses identified in the *parviglumis* rhizobiome ranged from 1.50 to 40.54 Kbp with 5 vOTUs and B73 viral contigs ranged from 1.51–31.18 Kbp with only 1 vOTU reconstructed. Viral contig clustering between two rhizobiomes resulted in the identification of only 7 (4.5%) viral contigs identified in both *parviglumis* and B73 (2 clustered >3 kb and 5 clustered <3 kb) (Fig. 4a). Rhizobiome viral community structure collected from each genotype was significantly different ($R^2 = 0.999$, $p = 0.005$) (Fig. 4b).

Taxonomy of rhizobiome viral contigs could be assigned to 38.80% in *parviglumis* and 30.23% in B73 viral contigs. Putative viruses were taxonomically associated with the Class Caudoviricetes. One unclassified archaeal dsDNA virus, Halovirus (3.84%

relative abundance), was present in the rhizobiome of B73 but was absent in the *parviglumis* rhizobiome. Over two-thirds of the viral contigs present could not be assigned.

Virus-host linkages

Virus-host linkages could be established for 31.34% of *parviglumis* and 36.04% of B73 viral contigs and vOTUs. Phyla Thermoproteota, Acidobacteriota, Actinobacteriota, and Patescibacteria were commonly identified in both genotypes and were associated with the highest number of viral contigs in *parviglumis* and B73 rhizobiome. Few viruses were coarsely associated with unclassified bacteria (4.76% in *parviglumis* and 9.67% in B73). Thermoproteota family Nitrososphaeraceae was the only archaeal host identified in the *Z. mays* rhizobiome. Of the identified hosts, 19.04% and 9.67% of viral contigs were linked to Nitrososphaeraceae in *parviglumis* and B73, respectively (Fig. 5a). Among the bacterial taxa Vicinamibacterales

a

b
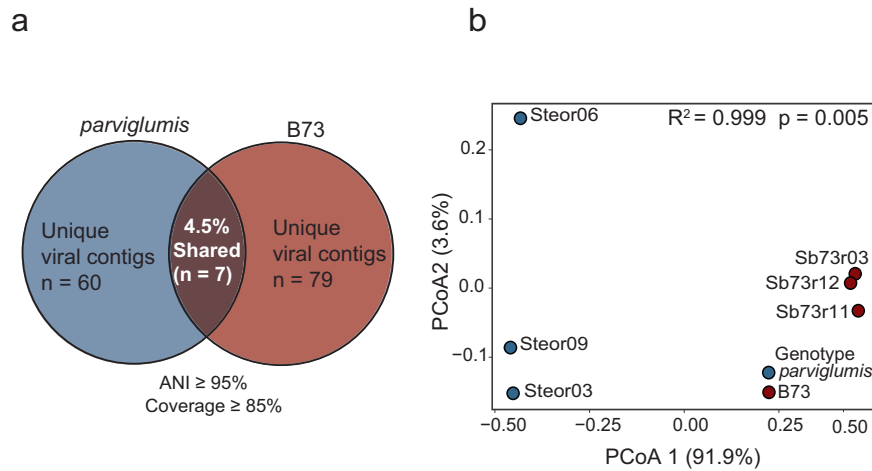
Fig. 4 Identification of viral contigs within the *parviglumis* and B73 rhizobiome. To assess the similarities/differences of viral contigs in the *parviglumis* and B73 rhizobiome, pairwise comparison with average nucleotide identity (ANI) ≥ 95% with coverage ≥ 85% of the viral contigs of the shorter sequence was performed where (**a**) only 7 viral contigs were clustered ≥ 95% ANI showing heterogeneity in identified viral contigs. **b** Ordination conducted with Bray-Curtis dissimilarity on the relative abundance of the viral contigs explained 91.9% variance on PCoA1 and 3.6% variance of $PCoA^2$ ($R^2 = 0.999$ $p = 0.005$) as analyzed by permutational multivariate analysis of variance (perMANOVA) conducted utilizing adonis2.

a   b   c
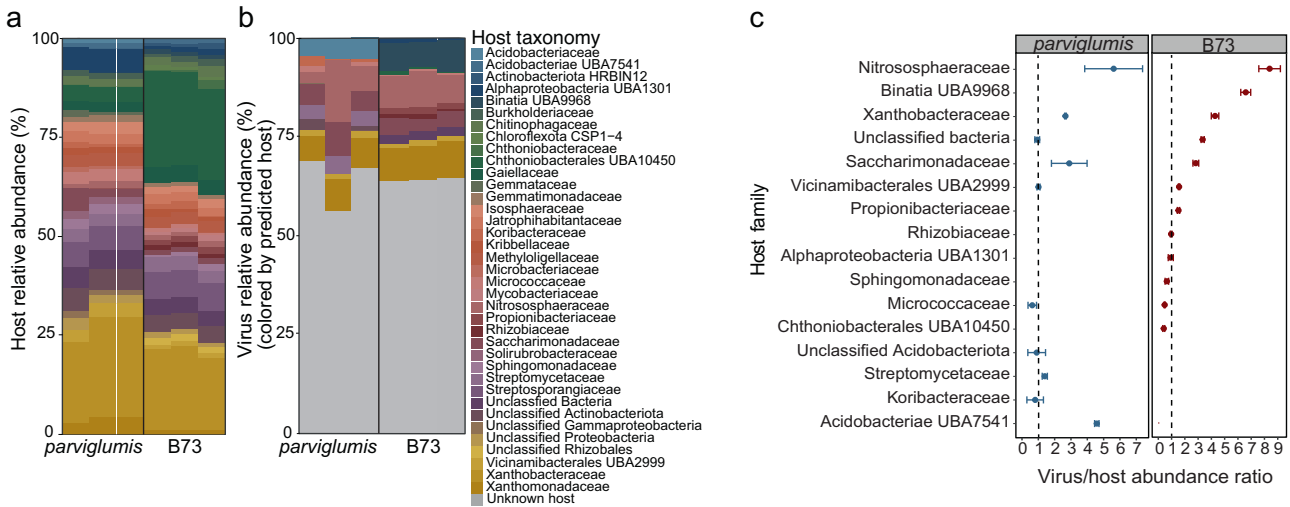
Fig. 5 Virus-host linkages identified in the *parviglumis* and B73 rhizobiome. a Relative abundance of microorganisms identified as hosts. **b** Viral contigs were linked to the hosts utilizing genome similarities, CRISPR sequences, and tetranucleotide frequencies between the metagenome-assembled genomes (MAGs) and viral contigs. While the hosts identified for the *parviglumis* and B73 viral contigs showed differences in the host preferences, hosts couldn't be identified for more than 60% of viral contigs in both genotypes and are represented in gray. The viral contigs are color-coded according to the identified potential hosts. **c** Virus to host abundance ratio was divided into 3 categories; less than 1, approximately 1, and greater than 1 demonstrated variation in viral genome copy number to their host in *parviglumis* and B73.The black vertical line separates the *Z. mays* genotypes, *parviglumis* and B73. The host taxonomy is identified at the family level (or lowest level of classification). Error bars represent the standard error of measure.

UBA2999, Micrococcaceae, Saccharimonadaceae, Xanthobacteraceae, and some unclassified bacteria were identified as common hosts in *parviglumis* and B73 (Fig. 5a). Viruses linked to Acidobacteriae UBA2999, Koribacteraceae, and Streptomycetaceae were unique to *parviglumis*. Rhizobiaceae, Propionibacteriaceae, Binatia UBA9968, Alphaproteobacteria UBA1301, Sphingomonadaceae, Chthoniobacterales UBA10450 were unique hosts in the rhizobiome of B73. None of the viral contigs were found to be infecting more than a single MAG in an established virus-host correlation indicating the virus host specificity. Verrucomicrobiota member Chthoniobacterales UBA10450 was highly abundant in the rhizobiome of both genotypes, it served as a virus host only in the B73 rhizobiome. Together these results indicated the variation of the community in the rhizobiome with host specificity.

A total of 64 and 98 putative CRISPR spacer regions were detected in *parviglumis* and B73 infected MAGs, respectively. Among all the identified CRISPR spacer sequences in both genotypes, only a single CRISPR spacer sequence provided a positive hit to one of the B73 MAGs. This corresponded to B73 MAG Xanthobacteraceae VAZQ01 sp005883115 with a 100% nucleotide identity match. The direct repeats flanking the CRISPR spacer region compared against the infected MAGs rendered an e-value < 10^{-10} confirming infection in Xanthobacteraceae VAZQ01 sp005883115 in B73 rhizobiome.

The ratio of viral contig and vOTUs (genome coverage) to host abundance as determined by MAG genome coverage ranged from 0.41 to 8.38 in rhizobiome *parviglumis* and B73. Viruses linked to Nitrososphaeraceae (Thermoproteota), Xanthobacteraceae

(Proteobacteria), and Saccharimonadaceae (Patescibacteria) exceeded host cells in both genotypes (Fig. 5b). Viruses linked to Vicinamibacterales UBA2999 (Acidobacteriota) equaled host cell abundance of in *parviglumis* but exceeded the linked host cells in the B73 rhizobiome. Viruses linked to the Micrococcaceae (Actinobacteriota) were lower in abundance than identified hosts in the rhizobiome collected from both genotypes. Viruses infecting Koribacteraceae (Acidobacteriota) in *parviglumis* and Chthoniobacterales UBA10450 (Verrucomicrobiota) in B73 were also lower than the linked host cell.

Metabolic potential of microbial and viral rhizobiome
The metabolic potential of the microbial community revealed the ability of the community to degrade carbohydrates as well as short chain fatty acids (Fig. 6). Bacterial hosts such as Xanthobacteraceae (Proteobacteria) not only showed the capability to degrade polyphenols, starch, short chain fatty acids, alcohols, chitins, and acetate utilization but were also capable of central carbon, nitrogen, sulfur, and iron metabolism (Fig. 6).

Host cells Acidobacteriota (Acidobacteriae UBA7541, Vicinamibacterales UBA2999, Koribacteraceae) and Actinobacteriota (Micrococcaceae, Propionibacteriaceae) harbored genes that associated with polysaccharide degradation enabling central carbon metabolisms such as glycolysis and the Kreb's cycle. Interestingly, the metabolic potential for CO_2 fixation, utilizing the dicarboxylate-hydroxybutyrate cycle, hydroxypropionate-hydroxybutylate cycle, and reductive citrate cycle (Arnon-Buchanan cycle) were identified in MAGs corresponding to archaea, Thermoproteota, and bacteria, Actinobacteriota, Bacteriodota, Proteobacteria, Verrucomicrobiota, in both genotypes. Genes associated with the Calvin Cycle were not identified in any of the MAGs. The metabolic potential to degrade polyphenol and cleavage of arabinan and fucose cleavage was restricted to the Koribacteraceae identified in the *parviglumis* rhizobiome (Fig. 6a). The ability to degrade chitin was specific to Desulfobacterota (Binatia UBA9968) and Verrucomicrobiota (Chthoniobacterales UBA10450) with the potential to degrade beta-mannan in the B73 rhizobiome (Fig. 6b). Archaeon Thermoproteota indicated the metabolic potential to convert acetate into methane, carbohydrate degradation and detoxification of aromatic compounds, and ammonia oxidation. Additionally, *parviglumis* MAGs Thermoproteota (Nitrososphaeraceae) and Proteobacteria (Xanthobacteraceae) were capable of denitrification. No B73 MAGs showed any role in nitrification and similarly, no *parviglumis* or B73 viral infected MAGs showed any role in sulfur metabolism. The microbial community in both *parviglumis* and B73 viral infected MAGs showed a role in siderophore transport to support iron acquisition in soils.

Putative AMGs were identified in one viral contig collected from the rhizobiome of B73 whereas putative AMGs were not identified in viral contigs recovered from *parviglumis*. Analysis of the viral encoded putative AMG identified this gene as a glycoside hydrolase family 5 (GH5). This virus was linked to the host Propionibacteriaceae (Actinobacteriota) in the B73 rhizobiome and carried putative AMGs capable of degrading amorphous cellulose, xyloglucan, xylan, beta-mannan, mixed-linkage glucans backbone cleavage, and chitin (Fig. 6b). The potential to degrade amorphous cellulose is redundant with the host whereas the AMGs associated with xyloglucan, xylan, beta-mannan, mixed-linkage glucans backbone cleavage, and chitin degradation potentially introduce additional metabolic function to the host. These results indicated that rhizobiome viruses can harbor genes with the potential to produce labile mono and oligosaccharides.

DISCUSSION
Here we demonstrated that both microbial and viral community structure varies between two *Z. mays* genotypes, *parviglumis* and B73, cultivated in the same homogenized soil under the same environmental conditions. While it is recognized the *Z. mays*

genotype influences the rhizosphere microbial community [72], to our knowledge this is the first study to demonstrate the variation of the rhizobiome viral community structure between plant genotypes. Plants release root exudates below ground, creating a diverse chemical milieu that impacts rhizobiome assemblage and structure [47, 73, 74]. The root exudate composition is also recognized to vary among maize genotypes [25], thus further promoting variation in the rhizosphere community. Our results are consistent with prior research demonstrating *Z. mays* genotype plays a factor influencing the selection of rhizobiome microbial community [72]. Here we identified Proteobacteria, Actinobacteriota, and Verrucomicrobiota constituted the microbiome of *parviglumis* and B73 consistent with a prior study [47] and were more abundant relative to the Acidobacteriota and Desulfobacterota. Interestingly, an abundance of viral contigs linked to Acidobacteria suggested the production of a higher number of viruses which could result in lower Acidobacterial cell abundance as a result of virus-mediated cell lysis. The relatively lower abundant microbial taxa in *Z. mays* rhizobiome such as Chloroflexota and Desulfobacterota (relative abundance <2.5% in 16S rRNA gene data) were reconstructed in B73, but we were unable to recover MAGs from *parviglumis*. This could be a result of low relative abundance and/or lysed host cells not detected in sequencing. Alternatively the result could be due to differential root-exudate production between genotypes [25] and recruitment of these taxa to the root. Microbial community structure and viral host cells are recognized to influence viral community structure [31, 75, 76]. Small but significant differences in rhizobiome microbial community composition in *parviglumis* and B73 manifested dramatic differences in the viral community of these two *Z. mays* genotypes.

Viruses were abundant in the rhizobiome of *parviglumis* and B73 rhizobiome outnumbering epifluorescent enumerated cells. The virus to cell ratio resulted in a VCR > 1.5, 3 times more than previously reported in the wheat rhizosphere (VCR = 0.27) [8]. Viral contigs recovered from the shotgun metagenome sequence data supported variation of the viral community between genotypes revealing the presence of a distinct viral community in the rhizobiome of *parviglumis* and B73. We recognize that members of the viral community composition reported in this study may represent an underestimate of viral diversity in the *Z. mays* rhizobiome due to sampling constraints because reported data in this study are limited to viruses associated with the host genome, adsorbed to particulate matter, and greater than 0.2 μm in size. Prior research has demonstrated significant variations in both microbial and viral community due to spatial distribution and/or soil heterogeneity [60, 77, 78], the close clustering of the *Z. mays* biological replicates on PCoA plot demonstrated that soil heterogeneity among replicates didn't contribute to significant differences in microbial and viral community structure. Rather the genotype of the plant played a significant role in the pronounced variation in the rhizobiome viral community where only seven viral contigs were shared between the two plant genotypes. This finding is also supported by pairwise comparison clustering of viral contigs which yielded only 7 similar viral contigs and validated that *parviglumis* and B73 comprised contrastingly different viral communities while grown in the same conditions using the same soil inoculum. Thus in addition to soil physiochemical factors, plant species and genotype can further contribute to the spatial variation of viral communities observed in soils.

Viral community variation in *parviglumis* and B73
Virus-host specificity and host range abundance plays an important role in viral selection in the rhizosphere [8]. The viral contigs recovered from the *parviglumis* and B73 rhizobiome revealed host specificity. All viral contigs recovered were found to infect a unique MAG. The strong correlation between cell and virus abundance is interconnected through prey-predator interactions. Repeated viral
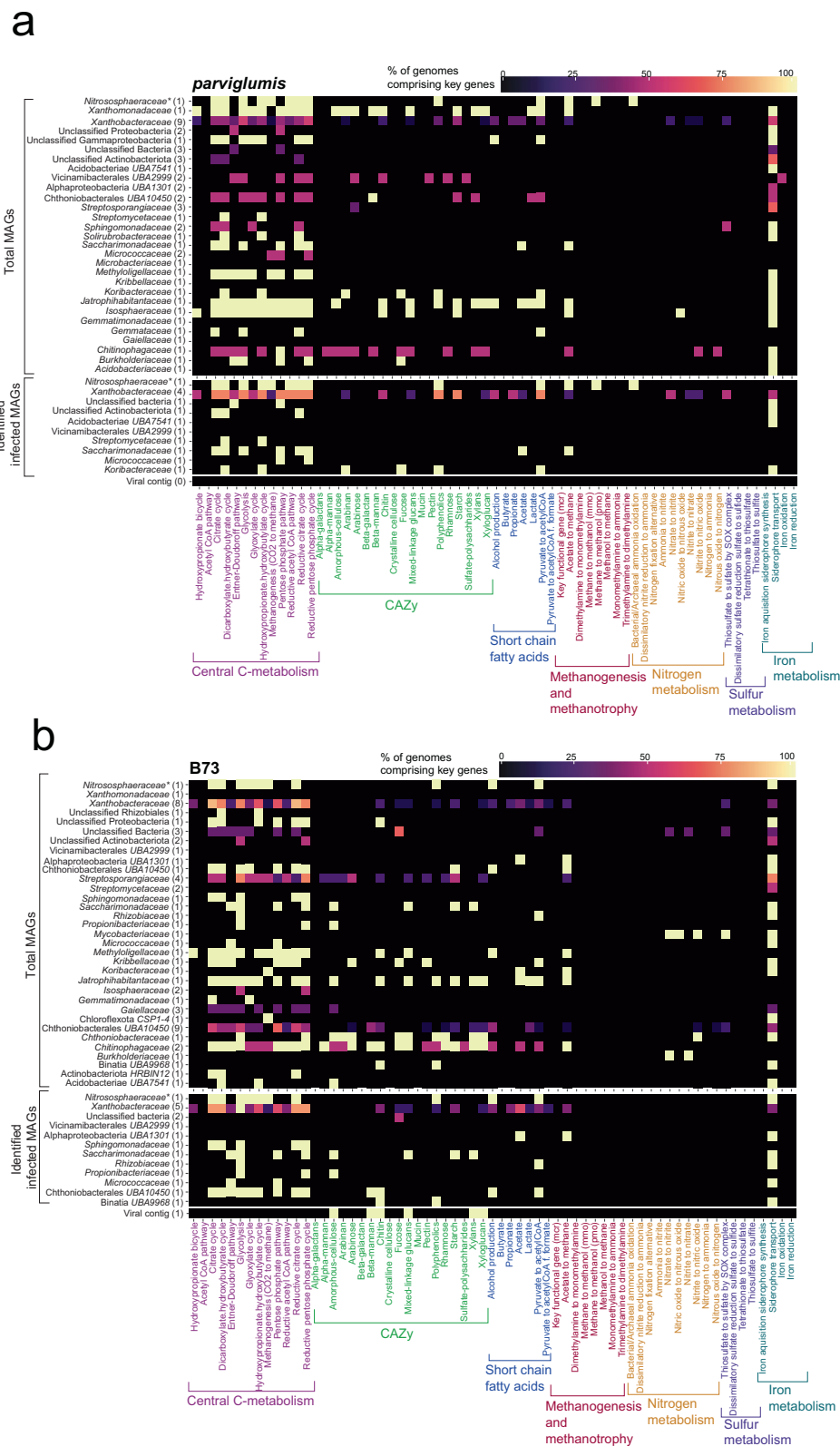
Fig. 6 Metabolic potential of the microbial community identified from the annotation of MAGs and virus contigs in the *parviglumis* and B73 rhizobiome. The rhizobiome metabolic potential was determined using DRAM, METABOLIC, and FeGenie. The heatmap represents the metabolic potential of the total metagenome-assembled genomes (MAGs) (top), viral infected MAGs (middle), and contribution of viral auxiliary metabolic genes (AMGs) (bottom) of (**a**) *parviglumis* and (**b**) B73 rhizobiome, respectively. Percentage of genomes were determined at the family level.

infections and host cell lysis give rise to virus-defense through immunity systems including the CRISPR-cas system found within some bacterial and archaeal lineages, thus, avoiding future viral infections [79]. The presence and 100% identity match to the CRISPR sequence in B73 MAG suggested the adaptation of a defense mechanism against viral infection by Xanthobacteraceae. This active defense mechanism of bacteria exploiting CRISPR sequences could be a possible explanation for the lower number of viral contigs in Xanthobacteraceae MAGs, hence, the high abundance of Xantho-bacteraceae in rhizobiome. The small genome size of the ultra-small bacteria Saccharimonadaceae (Patescibacteria) may not be able to comprise CRISPR sequences, thus rendering that cells are more susceptible to viral infection [80, 81]. However, the Patescibacteria adopted the strategy to evade viral infection by deleting common membrane phage protein receptors [82]. In contrast to these findings, we detected virus-host linkages in *Patescibacteria* [4, 76, 83, 84]. Viral predation results in altered community structure [85], can increase the release of biologically available nutrients, and can consequently impact ecosystem productivity [86]. Here we observed rhizobiome viral contigs linked to the host cells which demonstrated host preference which could subsequently impact host abundance as demonstrated by the variation in the ratio of viruses abundance to host abundance. Viral infection found to be impacting host metabolic output not only by impacting host abundance but also through acquiring putative glycoside hydro-lases AMG capable of complex polysaccharide degradation [15].

Impact of virus-host interactions on metabolic potential

Viruses can cause viral-mediated cell lysis liberating labile sources of carbon and nutrients [87] which can stimulate microbial population growth from the bottom up potentially altering community diversity and metabolic output [88, 89]. In a stable isotope probing (SIP) study performed in soils, the phyla Acidobacteriota, Actino-bacteriota, Chloroflexota, Proteobacteria, Patescibacteria, Verruco-microbiota were identified as active viral hosts involved in soil carbon cycling [81]. Taxa identified in our study were also identified to harbor the metabolic potential to play a role in carbon cycling within the roots. Genes associated with the metabolic potential to drive carbon oxidation and fermentation as well as carbon dioxide fixation (reductive citric acid cycle) were identified in the rhizobiome. Acidobacteriota (Acidobacteriae UBA7541, Vicinami-bacterales UBA2999, Koribacteraceae), Actinobacteriota (Micrococ-caceae, Propionibacteriaceae, Streptomycetaceae), Patescibacteria (Saccharimonadaceae), Proteobacteria (Alphaproteobacteria UBA1301, Sphingomonadaceae, Rhizobiaceae, Xanthobacteraceae), Verrucomicrbiota (Chthoniobacterales UBA10450), with the addi-tion archaeon Thermoproteota (Nitrososphaeraceae) showed potential to metabolize carbon through central carbon metabolism pathways. In addition to carbon biogeochemical cycling, members of the rhizobiome of both *parviglumis* and B73 had the potential for siderophore transport to support iron acquisition in soils. We did not detect the metabolic potential for nitrification and sulfur metabo-lism within taxa that were infected by viruses.

Viral encoded glycoside hydrolases putative AMGs have the potential to contribute to carbon metabolism in *Z. mays* rhizobiome through expression within the host cells. Here we observed the unclassified vOTU in the B73 rhizosphere that contained a glycoside hydrolase (GH5) which is recognized to degrade amorphous cellulose, beta-mannan, chitin, mixed-linkage glucans, xylans, and xyloglucan. The acquisition of the putative AMG, glycoside hydrolases responsible for carbohydrate hydro-lysis, by soil viruses is consistent with prior studies [15, 35, 81, 90] and demonstrates the metabolic potential within the rhizobiome. This vOTU that was linked to host Propionibacteriaceae (Actino-bacteriota) that respond to a variety of carbon sources by secreting extracellular enzymes such as cellulases, amylases, and chitinases were found to be regulating carbohydrate catabolic pathways [91, 92]. These results indicate that virus-encoded glycoside hydrolases have the potential to contribute to the production of labile mono- and oligosaccharides which can further serve as a carbon source for the host and other rhizobiome community members.

CONCLUSION

Together these results indicated that plant genotype plays a role in microbial assemblage in rhizobiome and viral community parallel shifts in response to microbial community selection. Viral community structure is linked to compositional patterns of microbial commu-nities based on plant genotypes. Thus, variation in below ground plant roots has the potential significantly influence heterogeneity of viruses within soils. The virus-host interaction showed differences in host abundance between two genotypes which has the capability to influence the metabolic potential of the rhizobiome. Putative viral AMGs have the potential to alter carbohydrate degradation and produce labile mono- and oligosaccharides in the rhizosphere. These labile carbon sources could further promote microbial community proliferation. Therefore, to extent to which host-virus interaction alters host abundance, microbial community structure, and functions remains a critical question in rhizosphere microbial ecology and soil biogeochemical cycling.

REFERENCES

1. Oburger E, Schmidt H. New methods to unravel rhizosphere processes. Trends Plant Sci. 2016;21:243–55.
2. Rout ME, Southworth D. The root microbiome influences scales from molecules to ecosystems: the unseen majority. Am J Bot. 2013;100:1689–91.
3. Pratama AA, Terpstra J, de Oliveria ALM, Salles JF. The role of rhizosphere bac-teriophages in plant health. Trends Microbiol. 2020;28:709–18.
4. Williamson KE, Fuhrmann JJ, Wommack KE, Radosevich M. Viruses in soil ecosystems: an unknown quantity within an unexplored territory. Ann Rev Virol. 2017;4:201–19.
5. Trubl G, Roux S, Solonenko N, Li YF, Bolduc B, Rodriguez-Ramos J, et al. Towards optimized viral metagenomes for double-stranded and single-stranded DNA viruses from challenging soils. PeerJ. 2019;7:e7265.
6. Williamson KE, Corzo KA, Drissi CL, Buckingham JM, Thompson CP, Helton RR. Estimates of viral abundance in soils are strongly influenced by extraction and enumeration methods. Biol Fert Soils. 2013;49:857–69.
7. Williamson KE, Radosevich M, Wommack KE. Abundance and diversity of viruses in six Delaware soils. Appl Environ Microbiol. 2005;71:3119–25.
8. Swanson MM, Fraser G, Daniell TJ, Torrance L, Gregory PJ, Taliansky M. Viruses in soils: morphological diversity and abundance in the rhizosphere. Ann Appl Biol. 2009;155:51–60.
9. Bi L, Yu DT, Du S, Zhang LM, Zhang LY, Wu CF, et al. Diversity and potential biogeochemical impacts of viruses in bulk and rhizosphere soils. Environ Microbiol. 2021;23:588–99.
10. Middelboe M, Jørgensen NO. Viral lysis of bacteria: an important source of dissolved amino acids and cell wall compounds. J Mar Biol Assoc UK. 2006;86:605–12.
11. Fuhrman JA. Marine viruses and their biogeochemical and ecological effects. Nature. 1999;399:541–8.
12. Suttle CA. Marine viruses–major players in the global ecosystem. Nat Rev Microbiol. 2007;5:801–12.
13. Wommack KE, Colwell RR. Virioplankton: viruses in aquatic ecosystems. Microbiol Mol Biol Rev. 2000;64:69–114.
14. Torsvik V, Ovreas L, Thingstad TF. Prokaryotic diversity–magnitude, dynamics, and controlling factors. Science (New York, NY). 2002;296:1064–6.
15. Emerson JB, Roux S, Brum JR, Bolduc B, Woodcroft BJ, Jang HB, et al. Host-linked soil viral ecology along a permafrost thaw gradient. Nat Microbiol. 2018;3:870–80.
16. Hurwitz BL, Hallam SJ, Sullivan MB. Metabolic reprogramming by viruses in the sunlit and dark ocean. Genome Biol. 2013;14:R123.
17. Kieft K, Zhou Z, Anderson RE, Buchan A, Campbell BJ, Hallam SJ, et al. Ecology of inorganic sulfur auxiliary metabolism in widespread bacteriophages. Nat Com-mun. 2021;12:1–16.

18. Wang S, Yang Y, Jing J. A synthesis of viral contribution to marine nitrogen cycling. Front Microbiol. 2022;13:834581.

19. Wu R, Smith CA, Buchko GW, Blaby IK, Paez-Espino D, Kyrpides NC, et al. Structural characterization of a soil viral auxiliary metabolic gene product–a functional chitosanase. Nat Commun. 2022;13:5485.

20. Zheng X, Jahn MT, Sun M, Friman V-P, Balcazar JL, Wang J, et al. Organochlorine contamination enriches virus-encoded metabolism and pesticide degradation associated auxiliary genes in soil microbiomes. ISME J. 2022;16:1397–408.

21. Li Y, Sun H, Yang W, Chen G, Xu H. Dynamics of bacterial and viral communities in paddy soil with irrigation and urea application. Viruses. 2019;11:347.

22. Edwards RA, Rohwer F. Viral metagenomics. Nat Rev Microbiol. 2005;3:504–10.

23. Kuske CR, Ticknor LO, Miller ME, Dunbar JM, Davis JA, Barns SM, et al. Comparison of soil bacterial communities in rhizospheres of three plant species and the interspaces in an arid grassland. Appl Environ Microbiol. 2002;68:1854–63.

24. Semchenko M, Xue P, Leigh T. Functional diversity and identity of plant genotypes regulate rhizodeposition and soil microbial activity. New Phytologist. 2021;232:776–87.

25. Lopez-Guerrero MG, Wang P, Phares F, Schachtman DP, Alvarez S, van Dijk K. A glass bead semi-hydroponic system for intact maize root exudate analysis and phenotyping. Plant methods. 2022;18:1–21.

26. Paterson E, Gebbing T, Abel C, Sim A, Telfer G. Rhizodeposition shapes rhizosphere microbial community structure in organic soil. New Phytol. 2007;173:600–10.

27. Bulgarelli D, Schlaeppi K, Spaepen S, Van Themaat EVL, Schulze-Lefert P. Structure and functions of the bacterial microbiota of plants. Annu Rev Plant Biol. 2013;64:807–38.

28. Srinivasiah S, Lovett J, Ghosh D, Roy K, Fuhrmann JJ, Radosevich M, et al. Dynamics of autochthonous soil viral communities parallels dynamics of host communities under nutrient stimulation. FEMS Microbiol Ecol. 2015;91:fiv063.

29. Ashelford KE, Day MJ, Bailey MJ, Lilley AK, Fry JC. In situ population dynamics of bacterial viruses in a terrestrial environment. Appl Environ Microbiol. 1999;65:169–74.

30. Ashelford KE, Norris SJ, Fry JC, Bailey MJ, Day MJ. Seasonal population dynamics and interactions of competing bacteriophages and their host in the rhizosphere. Appl Environ Microbiol. 2000;66:4193–9.

31. Brum JR, Ignacio-Espinoza JC, Roux S, Doulcier G, Acinas SG, Alberti A, et al. Patterns and ecological drivers of ocean viral communities. Science. 2015;348:1261498.

32. Santos-Medellin C, Estera-Molina K, Yuan M, Pett-Ridge J, Firestone MK, Emerson JB. Spatial turnover of soil viral populations and genotypes overlain by cohesive responses to moisture in grasslands. Proc Natl Acad Sci USA. 2022;119:e2209132119.

33. Trubl G, Solonenko N, Chittick L, Solonenko SA, Rich VI, Sullivan MB. Optimization of viral resuspension methods for carbon-rich soils along a permafrost thaw gradient. PeerJ. 2016;4:e1999.

34. Lee S, Sorensen JW, Walker RL, Emerson JB, Nicol GW, Hazard C. Soil pH influences the structure of virus communities at local and global scales. Soil Biol Biochem. 2022;166:108569.

35. Trubl G, Jang HB, Roux S, Emerson JB, Solonenko N, Vik DR, et al. Soil viruses are underexplored players in ecosystem carbon processing. MSystems. 2018;3:e00076–00018.

36. Gerba CP. Applied and theoretical aspects of virus adsorption to surfaces. Adv Appl Microbiol. 1984;30:133–68.

37. Strable J, Scanlon MJ. Maize (Zea mays): a model organism for basic and applied research in plant biology. Cold Spring Harbor protocols. 2009;2009:pdb.emo132.

38. Quattrone A, Lopez-Guerrero M, Yadav P, Meier MA, Russo SE, Weber KA. Interactions between root hairs and the soil microbial community affect the growth of maize seedlings. Plant Cell Environ. 2023;1–18. https://doi.org/10.1111/pce.14755.

39. Wolf DC, Skipper HD. Soil sterilization. In: Weaver RW, Angle S, Bottomley P, Bezdicek D, Smith S, Tabatabai A et al. (eds). *Methods of Soil Analysis: Part 2 Microbiological and Biochemical Properties*. Soil Science Society of America, Inc.: Madison, Wisconsin.1994: pp 41–51.

40. Hoagland DR, Arnon DI. The water-culture method for growing plants without soil. Document Number; California Agricultural Eexperiment Station, 1950:Circular-347

41. Wommack KE, Williamson KE, Helton RR, Bench SR, Winget DM. Methods for the isolation of viruses from environmental samples. Methods Mol Biol. 2009;501:3–14.

42. Pan D, Watson R, Wang D, Tan ZH, Snow DD, Weber KA. Correlation between viral production and carbon mineralization under nitrate-reducing conditions in aquifer sediment. ISME J. 2014;8:1691–703.

43. Pan D, Nolan J, Williams KH, Robbins MJ, Weber KA. Abundance and distribution of microbial cells and viruses in an alluvial aquifer. Front Microbiol. 2017;8:1199.

44. Westrop JP, Yadav P, Nolan P, Campbell KM, Singh R, Bone SE, et al. Nitrate-stimulated release of naturally occurring sedimentary uranium. Environ Sci Technol. 2023;57:4354–66.

45. Griffiths RI, Whiteley AS, O'Donnell AG, Bailey MJ. Rapid method for coextraction of DNA and RNA from natural environments for analysis of ribosomal DNA-and rRNA-based microbial community composition. Appl Environ Microbiol. 2000;66:5488–91.

46. Gilbert JA, Jansson JK, Knight R. The Earth Microbiome project: successes and aspirations. BMC Biol. 2014;12:1–4.

47. Peiffer JA, Spor A, Koren O, Jin Z, Tringe SG, Dangl JL, et al. Diversity and heritability of the maize rhizosphere microbiome under field conditions. P Natl Acad Sci USA. 2013;110:6548–53.

48. Callahan BJ, McMurdie PJ, Rosen MJ, Han AW, Johnson AJA, Holmes SP. DADA2: high-resolution sample inference from Illumina amplicon data. Nat Methods. 2016;13:581–3.

49. McMurdie PJ, Holmes S. phyloseq: an R package for reproducible interactive analysis and graphics of microbiome census data. PLos One. 2013;8:e61217.

50. Li D, Liu C-M, Luo R, Sadakane K, Lam T-W. MEGAHIT: an ultra-fast single-node solution for large and complex metagenomics assembly via succinct de Bruijn graph. Bioinformatics. 2015;31:1674–6.

51. Kang DD, Li F, Kirton E, Thomas A, Egan R, An H, et al. MetaBAT 2: an adaptive binning algorithm for robust and efficient genome reconstruction from metagenome assemblies. PeerJ. 2019;7:e7359.

52. Wu Y-W, Simmons BA, Singer SW. MaxBin 2.0: an automated binning algorithm to recover genomes from multiple metagenomic datasets. Bioinformatics. 2016;32:605–7.

53. Alneberg J, Bjarnason BS, de Bruijn I, Schirmer M, Quick J, Ijaz UZ, et al. Binning metagenomic contigs by coverage and composition. Nat Methods. 2014;11:1144–6.

54. Sieber CM, Probst AJ, Sharrar A, Thomas BC, Hess M, Tringe SG, et al. Recovery of genomes from metagenomes via a dereplication, aggregation and scoring strategy. Nat Microbiol. 2018;3:836–43.

55. Parks DH, Imelfort M, Skennerton CT, Hugenholtz P, Tyson GW. CheckM: assessing the quality of microbial genomes recovered from isolates, single cells, and metagenomes. Genome R. 2015;25:1043–55.

56. Eren AM, Esen ÖC, Quince C, Vineis JH, Morrison HG, Sogin ML, et al. Anvi'o: an advanced analysis and visualization platform for 'omics data. PeerJ. 2015;3:e1319.

57. Guo J, Bolduc B, Zayed AA, Varsani A, Dominguez-Huerta G, Delmont TO, et al. VirSorter2: a multi-classifier, expert-guided approach to detect diverse DNA and RNA viruses. Microbiome. 2021;9:1–13.

58. Ren J, Song K, Deng C, Ahlgren NA, Fuhrman JA, Li Y, et al. Identifying viruses from metagenomic data using deep learning. Quant Biol. 2020;8:64–77.

59. Jarett JK, Džunková M, Schulz F, Roux S, Paez-Espino D, Eloe-Fadrosh E, et al. Insights into the dynamics between viruses and their hosts in a hot spring microbial mat. ISME J. 2020;14:2527–41.

60. Santos-Medellin C, Zinke LA, Ter Horst AM, Gelardi DL, Parikh SJ, Emerson JB. Viromes outperform total metagenomes in revealing the spatiotemporal patterns of agricultural soil viral communities. ISME J. 2021;15:1956–70.

61. Roux S, Adriaenssens EM, Dutilh BE, Koonin EV, Kropinski AM, Krupovic M, et al. Minimum Information about an Uncultivated Virus Genome (MIUViG). Nature Biotechnology. 2019;37:29–37.

62. Starr EP, Shi S, Blazewicz SJ, Probst AJ, Herman DJ, Firestone MK, et al. Stable isotope informed genome-resolved metagenomics reveals that Saccharibacteria utilize microbially-processed plant-derived carbon. Microbiome. 2018;6:1–12.

63. Barrangou R, Fremaux C, Deveau H, Richards M, Boyaval P, Moineau S, et al. CRISPR provides acquired resistance against viruses in prokaryotes. Science. 2007;315:1709–12.

64. Paez-Espino D, Eloe-Fadrosh EA, Pavlopoulos GA, Thomas AD, Huntemann M, Mikhailova N, et al. Uncovering Earth's virome. Nature. 2016;536:425–30.

65. Roux S, Brum JR, Dutilh BE, Sunagawa S, Duhaime MB, Loy A, et al. Ecogenomics and potential biogeochemical impacts of globally abundant ocean viruses. Nature. 2016;537:689–93.

66. Ahlgren NA, Ren J, Lu YY, Fuhrman JA, Sun F. Alignment-free oligonucleotide frequency dissimilarity measure improves prediction of hosts from metagenomically-derived viral sequences. Nucleic Acids R. 2017;45:39–53.

67. Ahlgren NA, Fuchsman CA, Rocap G, Fuhrman JA. Discovery of several novel, widespread, and ecologically distinct marine Thaumarchaeota viruses that encode amoC nitrification genes. ISME J. 2019;13:618–31.

68. Zhou Z, Tran PQ, Breister AM, Liu Y, Kieft K, Cowley ES, et al. METABOLIC: High-throughput profiling of microbial genomes for functional traits, biogeochemistry, and community-scale metabolic networks. Microbiome. 2022;10:33.

69. Shaffer M, Borton MA, McGivern BB, Zayed AA, La Rosa SL, Solden LM, et al. DRAM for distilling microbial metabolism to automate the curation of microbiome function. Nucleic acids research. 2020;48:8883–8900.

70. Garber AI, Nealson KH, Okamoto A, McAllister SM, Chan CS, Barco RA, et al. FeGenie: a comprehensive tool for the identification of iron genes and iron gene neighborhoods in genome and metagenome assemblies. Front Microbiol. 2020;11:37.

71. Author. Vegan: Community Ecology Package. R package. https://CRAN.R-project.org/package=vegan (2017).

72. Bouffaud M-L, Kyselková M, Gouesnard B, Grundmann G, Muller D, Moënne-Loccoz Y. Is diversification history of maize influencing selection of soil bacteria by roots? Mol Ecol. 2012;21:195–206.

73. Badri DV, Vivanco JM. Regulation and function of root exudates. Plant Cell Environ. 2009;32:666–81.

74. Zhalnina K, Louie KB, Hao Z, Mansoori N, da Rocha UN, Shi S, et al. Dynamic root exudate chemistry and microbial substrate preferences drive patterns in rhizo-sphere microbial community assembly. Nat Microbiol. 2018;3:470–80.

75. Liang X, Wang Y, Zhang Y, Zhuang J, Radosevich M. Viral abundance, community structure and correlation with bacterial community in soils of different cover plants. Appl Soil Ecol. 2021;168:104138.

76. Sandaa, E. Storesund R-A, Olesin E J, Lund Paulsen M, Larsen A, Bratbak G, et al. Seasonality drives microbial community structure, shaping both eukaryotic and prokaryotic host–viral relationships in an arctic marine ecosystem. Viruses. 2018;10:715.

77. Hutchings MJ, John EA, Wijesinghe DK. Toward understanding the consequences of soil heterogeneity for plant populations and communities. Ecology. 2003;84:2322–34.

78. Roux S, Emerson JB. Diversity in the soil virosphere: to infinity and beyond? Trends Microbiol. 2022;30:1025–35.

79. Burstein D, Sun CL, Brown CT, Sharon I, Anantharaman K, Probst AJ, et al. Major bacterial lineages are essentially devoid of CRISPR-Cas viral defence systems. Nat Commun. 2016;7:1–8.

80. Tian R, Ning D, He Z, Zhang P, Spencer SJ, Gao S, et al. Small and mighty: adaptation of superphylum Patescibacteria to groundwater environment drives their genome simplicity. Microbiome. 2020;8:1–15.

81. Trubl G, Kimbrel JA, Liquet-Gonzalez J, Nuccio EE, Weber PK, Pett-Ridge J, et al. Active virus-host interactions at sub-freezing temperatures in Arctic peat soil. Microbiome. 2021;9:1–15.

82. Tian R, Ning D, He Z, Zhang P, Spencer SJ, Gao S, et al. Small and mighty: adaptation of superphylum Patescibacteria to groundwater environment drives their genome simplicity. Microbiome. 2020;8:51.

83. Liang X, Zhang Y, Wommack KE, Wilhelm SW, DeBruyn JM, Sherfy AC, et al. Lysogenic reproductive strategies of viral communities vary with soil depth and are correlated with bacterial diversity. Soil Biol Biochem. 2020;144:107767.

84. Brum JR, Hurwitz BL, Schofield O, Ducklow HW, Sullivan MB. Seasonal time bombs: dominant temperate viruses affect Southern Ocean microbial dynamics. ISME J. 2016;10:437–49.

85. Thingstad TF, Våge S, Storesund JE, Sandaa R-A, Giske J. A theoretical analysis of how strain-specific viruses can control microbial species diversity. P Natl Acad Sci USA. 2014;111:7813–8.

86. Suttle CA. Viruses in the sea. Nature. 2005;437:356–61.

87. Tong D, Wang Y, Yu H, Shen H, Dahlgren RA, Xu J. Viral lysing can alleviate microbial nutrient limitations and accumulate recalcitrant dissolved organic matter components in soil. ISME J. 2023;17:1247–56.

88. Middelboe M, Lyck PG. Regeneration of dissolved organic matter by viral lysis in marine microbial communities. Aquat Microb Ecol. 2002;27:187–94.

89. Liang C, Schimel JP, Jastrow JD. The importance of anabolism in microbial control over soil carbon storage. Nat Microbiol. 2017;2:1–6.

90. Starr EP, Shi S, Blazewicz SJ, Koch BJ, Probst AJ, Hungate BA, et al. Stable-isotope-informed, genome-resolved metagenomics uncovers potential cross-kingdom interactions in rhizosphere soil. Msphere. 2021;6:e00085–00021.

91. Genilloud, O. Physiology of actinobacteria. In: Wink J, Mohammadipanah F, Hamedi J (eds). *Biology and Biotechnology of Actinobacteria*. Springer: Cham, Switzerland. pp 151-80 (2017).

92. Singh PR, Jain M. Studies on the cellulolytic bacteria and cellulose degradation in a cattle waste-fed biogas digester. MIRCEN J Appl Microbiol Biotechnol. 1986;2:309–17.

AUTHOR CONTRIBUTIONS
PY and KAW designed the study. PY, AQ, YY, TK, SER, and KAW developed the data collection protocols. PY, AQ, YY, TK, JO, RK, SER, and KAW conducted the experiment and collected the data. PY and KAW analysed the data, with help from SER and AQ, PY and KAW wrote the initial draft. All authors edited the manuscript.

COMPETING INTERESTS
The authors declare no competing interests.

ADDITIONAL INFORMATION
Supplementary information The online version contains supplementary material available at https://doi.org/10.1038/s43705-023-00335-4.

Correspondence and requests for materials should be addressed to Karrie A. Weber.

Reprints and permission information is available at http://www.nature.com/reprints

Publisher's note Springer Nature remains neutral with regard to jurisdictional claims in published maps and institutional affiliations.